Insights into the non-covalent interactions of hydrogen sulfide with fenchol and fenchone from a gas-phase rotational study

Noureddin Osseiran, Elias M Neeman, Pascal Dréan, Manuel Goubet, Thérèse R Huet

Insights into the non-covalent interactions of hydrogen sulfide with fenchol and fenchone from a gas-phase rotational study

Noureddin Osseiran,[a] Elias M. Neeman,[a] Pascal Dréan,[a] Manuel Goubet,[a] and Thérèse R. Huet [*a]

[a] Univ. Lille, CNRS, UMR 8523 – PhLAM – Physique des Lasers Atomes et Molécules F-59000 Lille, France. Email : therese.huet@univ-lille.fr

The gas-phase non-covalent interactions in the endo-fenchol-H_2S and fenchone-H_2S complexes have been unveiled using rotational spectroscopy in a supersonic jet expansion, and quantum chemical calculations. In *endo*-fenchol, the hydrogen bond HSH···OH together with dispersive interactions stabilizes the system. In fenchone, the weak interaction HSH···O=C allows an internal dynamic of H_2S.

Biogenic Volatile Organic compounds (BVOCs) are naturally present in the atmosphere, due to emission by vegetation. Monoterpenes and terpenoids, which are formed by a combination of two or more isoprene units, represent 11% of the total BVOCs global emissions rate (760 TgC per year).[1] They can oxidize to a range of products that contribute to secondary organic aerosols (SOA) formation, which in turn alter physical and chemical processes in the atmosphere, thus affecting climate and human health.[2] SOA formation is not fully understood, but it has been shown to be provoked by humidity, where aerosol concentration increase with increased humidity.[3] Thus, it is relevant to study the interactions between solute and water. It is nowadays well established that Fourier transform microwave (FTMW) spectroscopy in jet-cooled conditions supported by theoretical calculations is a powerful technique to study the hydrogen bonded (HB) systemsr.[4–6]

Among minor atmospheric compounds, hydrogen sulphide (H_2S) is a gas that can be found globally in the atmosphere with natural emissions rate estimated at 4.4 Tg per year.[7] It is emitted from natural and anthropogenic sources. Examples of its natural sources are volcanoes and wetlands, whereas livestock production and industrial processes (e.g., fossil fuels combustion) are considered anthropogenic sources.[7,8] H_2S can play an important role in shaping Earth's atmosphere. Only recently, the H_2S dimer in the gas phase has been shown to have a similar structure to that of the water dimer.[9] Noticeably, few experimental investigations have been performed to evidence the hydrogen bond complex between H_2S and organic molecules, such as $C_6H_6\cdots H_2S$[10] and $C_6H_5CCH\cdots H_2S$,[11] while HB with water is extensively studied. In this context, the relevance of studying complexes of monoterpenoids with H_2S, and comparing it to water, is obvious. Indeed, the ability of H_2S to form HB with organic compounds is very little known, particularly fundamental properties such as solvation sites and the nature of the interactions involved in the solvation energy. To pave the way for answers to these questions, we have examined the HB between H_2S and two similar bicyclic chiral molecules of atmospheric interest, but having two different functional groups: a ketone (C=O) and alcohol (C-OH). The two chosen terpenoids are endo-fenchol ($C_{10}H_{18}O$, 1,3,3-trimethylbicyclo[2.2.1]heptan-2-ol, labelled as EF) and fenchone ($C_{10}H_{16}O$, 1,3,3-trimethylbicyclo[2.2.1]heptan-2-one, labelled as FEN). Both having the same bicyclic unit, the functional group influence on the HB with H_2S can be investigated. The hydration of both EF and FEN molecules (i.e. HB with water) was previously studied.[12,13] Both molecules showed relatively different hydration properties. For EF, only one monohydrate has been observed and the presence of a water molecule was found to alter the orientation of the hydroxyl group.[12] FEN is more capable of forming complexes with water, as several monohydrates, dihydrates, and trihydrates have been reported, without significant alteration of its most stable structure.[13]

In this communication, we present the successful identification of the 1:1 complex of EF and FEN with H_2S, based on the interplay between theoretical methods and experiments. Such a comprehensive study uses a combination of three different quantum chemical calculation methods with high-resolution rotational spectroscopy.

Calculation details are reported in the ESI. The structures of the possible most stable conformers of EF-H_2S and FEN-H_2S have been optimized using *ab initio* calculations, i.e., MP2 (Møller–Plesset second-order perturbation theory) and density-functional theory (DFT) methods (wB97X-D and B3LYP) combined with different combinations of basis sets (see ESM for details). For EF-H_2S four low energy conformers have been predicted, all the EF conformers attach to the H_2S molecule by a weak hydrogen bond (see Figure S3 for the structures of the

obtained minima). It is worth noting that the H_2S induces also an alteration in the structure of EF as in the case of EF-H_2O, where the orientation of the hydroxyl group in the most stable complexes does not match that of the most stable EF monomer. For FEN-H_2S, six low energy conformers have been predicted by theoretical calculations, whose structures differ than those observed in the case of water (see Figure S4 for the structures of the obtained minima). Sulfur is less electronegative than oxygen and consequently forms a week HB in this system which results in a flexible complex system that permits the outer (free) hydrogen of H_2S to lay from either side of the HB plane (O – bonded-H – S plane), increasing the number of possible low energy structures. Due to the small differences between the relative energies of the predicted conformers (< 0.5 kJ mol^{-1}), multiple conformers can be expected to be observed in the molecular-jet expansion. After considering all the calculated structures, the experiments were performed using cavity-based Fourier transform microwave (FP-FTMW) spectrometers operating in the 2-20 GHz.[14] Experimental details are reported in the ESM, only a brief description of the methodology is given here. A commercial sample of EF (and FEN) was introduced into the nozzle reservoir and heated to about 350 K. Sample vapor was then seeded in a gas mixture consisting of about 1.5 % H_2S diluted in neon carrier gas at a stagnation pressure of 4 bars. All the conformers of EF-H_2S and FEN-H_2S are predicted to have a spectrum dominantly of a-type. Consequently, an initial search and assignment of a-type transitions was successful after several trials. All fits were performed using the SPFIT/SPCAT suite of programs.[15]

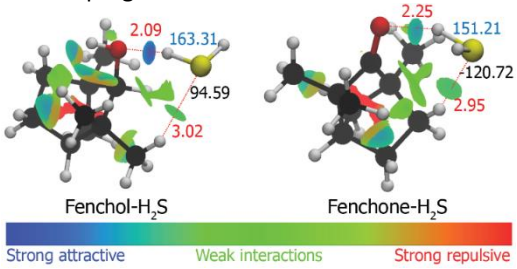

Fig. 1 The NCI iso-surfaces show strong attractive HB (blue) in the case of EF-H_2S (left), and weaker HB in the case of FEN-H_2S (right) in the observed species IIIEF and IVFEN respectively. Distances (Å) are shown in red. The OHS and the OHSH angles values are indicated in blue and in black, respectively.

Fig. 1 presents the observed 1:1 complexes, and the map of the Non-Covalent Interactions (NCI) analysis (see discussion). The rotational molecular parameters are given in Table 1 and compared to calculations at the MP2/6-311++G(d,p) level, considered to have good reliability. All other calculations results are presented in the ESM. For EF-H_2S, one conformer has been observed, and 56 a-type transitions were measured. The identified rotational transitions were fitted to a Watson semi-rigid Hamiltonian in the A reduction and I^r representation (see Table 1).[16]

The identification of the observed species can be made by comparing the experimental and theoretical constants.

Conformers II_{EF} and III_{EF} have too similar rotational constants (few MHz) and energies (few tenths of kJ mol^{-1}) to be discerned, but their different projections of the permanent dipole moment on the principal inertia axes can be used complementarily (see $|\mu_a|$, $|\mu_b|$ and $|\mu_c|$ in Table 1). Indeed, the observation of only a-type transitions allows the unambiguous identification of the observed species as conformer III_{EF}. No extra unknown lines indicating the presence of other conformers have been observed despite of our search for them. This can be due either to very weak undetectable signals or to relaxation in the jet. For FEN-H_2S species, only one conformer has also been observed, all the observed lines were assigned, to a-type, b-type and c-type transitions. Those observed lines were found split into two component states showing an intensity ratio of 3:1. Such ratio corresponds to the statistical weight expected for the internal rotation of H_2S around its C_2 symmetry axis, which implies the exchange of a pair of equivalent hydrogen atoms (fermions).

The energy states involved in weak and strong components of transitions were denoted as 0^+ and 0^-, respectively. The measured transitions were fitted to the same semi-rigid Hamiltonian mentioned above and it was used to fit the two series of transitions separately (see Table 1). Similar to the case of EF-H_2S, the are very small difference in energies between the first four conformers, which falls within the error range of the calculations. Also, the rotational constants of III_{FEN} and IV_{FEN} are very close which prevents a straightforward assignment. The rotational constants of the conformers I_{FEN} and II_{FEN} were farther away from the experimental values and thus they were excluded from the assignment. To identify the observed species of FEN-H_2S, we compare the experimental microwave power used to optimize each type (a, b or c) of transitions. The projections of the dipole moment components for the conformer III_{FEN} are expected to be on the order of $\mu_a > \mu_b \approx \mu_c$, whereas for IV_{FEN} the order is $\mu_a > \mu_c > \mu_b$. Experimentally, b-type transitions are observed roughly four times smaller than c-type transitions and roughly six times smaller than a-type transitions. These observations are consistent with the case of IV_{FEN} and can confirm the assignment of IV_{FEN} as the observed species. No extra unknown lines indicating the presence of other conformers have been observed despite of our search for them.

Noticeably, no tunneling splitting was observed in previously studied complexes of terpenoids with H_2O,[12,13] calling for further investigations of the behavior of H_2S in the case of FEN by starting from the identification of the internal motion causing it. A possible motion could be the wedging of H_2S connecting the two conformers III_{FEN} and IV_{FEN}. However, it would not correspond to a proton exchange with a 1:3 statistical weight. In addition, a flip of the free H atom would give rise to a variation of the rotational constants of several hundreds of kHz, as confirmed by our calculations, while our two sets of experimental constants display a difference of one order of magnitude smaller (see Table 1). The only movement connecting two equivalent minima by exchanging protons is the internal rotation of H_2S around its C_2 axis. The potential energy pathway for the internal rotation was investigated at the

Table 1 Values of the rotational parameters and electric dipole moment components for the observed and calculated EF-H_2S and FEN-H_2S conformers, at the MP2/6-311++G(d,p) level of theory. Only conformers below 4 kJ mol^{-1} are considered.

	EF-H_2S					FEN-H_2S					
	Exp.	I_{EF}	II_{EF}	III_{EF}	IV_{EF}	0^+	0^-	I_{FEN}	II_{FEN}	III_{FEN}	IV_{FEN}
A[a]	1161.2329(32)	992.1	1187.5	1182.5	993.9	983.41497(21)	983.40341(13)	1092.9	1091.5	984.2	985.1
B	494.21434(11)	564.6	510.2	505.8	566.5	582.232474(64)	582.241521(34)	610.7	610.4	597.2	599.0
C	430.006772(86)	491.9	445.3	439.5	492.6	511.016389(44)	511.007220(30)	507.2	506.6	525.1	526.9
Δ_J	0.20603(35)	0.0867	0.1213	0.0553	0.0761	0.18499(14) [g]		0.1136	0.1288	0.1214	0.1091
Δ_K	-0.4525 [b]	-0.4211	0.0580	-0.4525	-0.6174	-1.6012(59)		-0.0362	-0.1155	-1.3961	-0.7291
Δ_{JK}	0.8615(31)	0.3675	0.1910	0.7496	0.5718	1.4868(14)		0.0192	0.1082	1.4238	0.6980
δ_J	0.03287(22)	0.0111	0.0208	0.0076	0.0095	0.015727(80)		0.0146	0.0157	0.0136	0.0101
δ_K	0.231(12)	0.1317	0.1466	0.2892	0.2354	0.7361(24)		0.0758	0.1124	0.6329	0.3034
$\lvert\mu_a\rvert$	Obs.	2.1	1.6	2.7	2.0	Obs. Intense		2.0	1.9	2.7	2.5
$\lvert\mu_b\rvert$	Not obs.	0.07	0.8	0.02	0.03	Obs. Weak		0.5	0.9	1.1	0.4
$\lvert\mu_c\rvert$	Not obs.	0.9	0.2	0.1	0.7	Obs. Medium		1.8	1.4	1.3	1.5
N[c]	56	-	-	-	-	70	99	-	-	-	-
σ[d]	1.44	-	-	-	-	1.72				-	-
ΔE_{ZPE}[e]	-	0.0	0.03	0.11	0.28	-		0.0	0.08	0.38	0.44
ΔG_{348}[f]	-	1.37	0.00	0.40	1.02	-		3.22	1.64	0.00	2.00

[a] A, B, and C are the rotational constants in MHz; Δ_J, Δ_{JK}, Δ_K, δ_J, and δ_K are the quartic centrifugal distortion in kHz; μ_a, μ_b, and μ_c are the electric dipole moment components in D. [b] The value is fixed to the MP2/6-311++G(d,p) value. [c] Number of fitted transitions. [d] rms deviation of the fit in kHz. [e] Relative energies (in kJ mol^{-1}) with respect to the global minimum, taking into account the zero point energy (ZPE) correction, at the MP2/6-311++G(d,p). [f] Gibbs free energies (348K). [g] The centrifugal distortion constants of the two states were constrained to have the same values in the fit.

MP2/6-311++G(d,p) level of theory and the barrier was estimated to be about 940 cm^{-1} (see SI).

Natural bond orbital (NBO) analysis provides an intuitive description of intermolecular interactions to rationalize the associated transfer of electronic charge.[17] The NBO analyses were performed using the MP2/6-311++G(d,p) method. The first general result of the NBO calculations is that the intermolecular interactions can be explained in terms of about 99% of Lewis structure and about 1% of non-Lewis structure. These values reflect an appreciable degree of charge delocalization in the intermolecular HB that stabilizes the structure. In both cases, this intermolecular interaction is formed between a lone pair (LP) of the oxygen atom and the anti-bonding (BD*) orbitals of the S-H bond pointing toward the former. Concerning conformer III_{EF}, the dominant interactions involve the two lone pairs (LP) of O_{EF}. The first, between LP(1) of O_{EF} and BD* of S-H, has a stabilization energy of 9.4 kJ mol^{-1} while the second, between LP(2) of O_{EF} and the same BD* of S-H, has a stabilization energy of 15.4 kJ mol^{-1} (see Fig. S5 of ESM). Due to obvious geometry features, LP(2) being the most aligned to HB direction has a larger impact than LP(1). In addition, the dispersive interaction between the LP(2) of S and BD* of the nearest C-H of EF is estimated to be about 3.3 kJ mol^{-1} (see Fig. S6 of ESM). It is small but not negligible to stabilize this structure, showing a sort of weak "secondary" HB. The structure of conformer III_{EF} is similar to that observed in the case of EF···H_2O, consequently, another interesting comparison can be made between H_2O and H_2S. The obvious observation is that the principal HB is stronger in the case of EF···H_2O (33.6 kJ mol^{-1}) but the secondary dispersive interaction is smaller (≈ 1.5 kJ mol^{-1}) and involves the two nearest hydrogens of the germinal methyl groups[12] instead of only the closest hydrogen in the case of EF-H_2S.

Similarly, the NBO analysis for IV_{FEN} shows an HB characterized by the interaction between LP(1) of O_{FEN} and BD* of S-H with stabilization energy of 3 kJ mol^{-1} (see Fig. S7 of ESM). An additional interaction occurs between the bonding orbital BD(2) of C=O and BD* of S-H with a stabilization energy of 5.6 kJ mol^{-1}. Likewise, a secondary interaction between LP(2) of S and BD* of the nearest C-H of FEN is calculated to be about 5.3 kJ mol^{-1} (see Fig. S8 of ESM). Therefore, from this NBO analysis, one can say that the large-amplitude motion of H_2S in the case of IV_{FEN} could be explained by the weakness of the HB involved in its stabilization which is about 3 times lower than its value in the case of III_{EF}. It correlates with the calculated HB structural difference whose length (S-H···O) is noticeably shorter in III_{EF} (2.092 Å) than that in IV_{FEN} (2.251 Å). Because of largely different structures, conformer IV_{FEN} could not be finely compared to any of the two observed structures of FEN···H_2O. Indeed, the water unit is placed next to the methyl groups of FEN while in the case of H_2S, it places itself perpendicularly next to the methylene of the FEN ring. However, the interaction energy in the case of IV_{FEN} is weaker than that of both observed 1:1 complexes with water (higher than 26 kJ mol^{-1}).[12]

To visualize the intermolecular interactions in both complexes with H_2S, Non-Covalent Interactions (NCI) analysis was performed.[18] To plot the map of the interactions involved in the stabilization of the observed conformers, NCI analysis was carried out using the NCIplot software[18] from the MP2/6-311++G(d,p) level calculations and visualized using the VMD program[19] as displayed in Fig. 1. NCI results confirm that the HB in the case of EF-H_2S, shown by an iso-surface in dark blue color, is stronger than that of FEN-H_2S, shown by an iso-surface in light

blue color. In addition, it shows the two additional weak interactions between the sulfur atom and the hydrogen of EF and FEN as shown by iso-surfaces in green color. These results are in perfect agreement with the NBO analysis.

To further confirm and understand the non-covalent interactions taking place, Symmetry-adapted perturbation theory (SAPT)[20] analyses were carried out. This method is used for energy decomposition analyses, where it provides the decomposition of the total interaction energy into electrostatic, exchange, induction, and dispersion energy terms. Calculations for the two complexes were performed at the $SAPT_{2+3}$ level based on the MP2/6-311++G(d,p) optimized geometries. Table 2 presents the calculated energy decompositions for the two complexes. It can be seen that the electrostatic contribution to the total energy in the EF-H_2S complex is higher than that in the FEN-H_2S complex. This provides another evidence that the HB with EF is stronger than with FEN, and one more explanation for the fact that tunneling splitting is only observed in the FEN-H_2S complex. Concerning the other terms, the relative contribution of the dispersion forces indicates that they are stronger in FEN-H_2S complex compared to the EF-H_2S complex. The ESI contains a radar chart showing the contribution of the different terms to the total energy, for the two complexes as well as their water analogs. The SAPT analysis results confirm the much stronger HB in the case of monohydrates. In any case, these interactions play a key role in the stabilization and preference within the conformational landscape of HB complexes.

Table 2 The calculated interaction and total energies of the two observed EF-H_2S and FEN-H_2S conformers, obtained at the $SAPT_{2+3}$ level.

Energy (kJ mol^{-1})	EF···H_2S	FEN···H_2S
Electrostatic	-29.23	-21.02
Exchange	42.69	31.02
Induction	-10.07	-6.87
Dispersion	-16.91	-15.95
Total	-13.53	-12.83

Conclusions

We performed the identification and characterization of the interaction of H_2S with endo-fenchol and fenchone and its comparison with water. The strong HB in EF-H_2S forms a rigid structure similar to the case of EF-H_2O. The much weaker HB in the case of FEN-H_2S leaves the H_2S unit dynamically quasi-free to rotate around its C_2 axis as evidenced by the observed tunneling splitting of the lines. In addition, FEN-H_2S is unique and very different from the two FEN-H_2O conformers. Noticeably, only one FEN complex was observed with H_2S while several mono-, di- and tri-hydrated complexes were evidenced. In all cases, structural parameters and quantitative intermolecular interaction estimations show a much stronger association with H_2O than with H_2S, suggesting that water is a much better micro-solvent than hydrogen sulfide. Although this is known in the condensed phase, it deserved an investigation in the gas phase at the molecular scale. At least, this indicates that sulfur behaves in a different way than oxygen in micro-solvation processes. Similarly, micro-solvation of the sp_3 hybridized oxygen in a hydroxyl functional group is stronger than that of the sp_2 hybridized oxygen in a ketone functional group, suggesting that hydroxyls are better solutes than ketones. The present study is a quantitative characterization of the HB of BVOCs atmospherically relevant with the minor compound H_2S, calling for the study of more complicated systems such as with more than one H_2S molecule and paving the way in the knowledge of the role of H_2S in SOA formation.

Acknowledgements

The present work was funded by the French ANR through the PIA under contract ANR-11-LABX-0005-01, by the Regional Council *Hauts-de-France*, by the European Funds for Regional Economic Development (FEDER), and by the CPER CLIMIBIO. It is a contribution to the scientific project Labex CaPPA. E. M. N. would like to thank the CNRS for a researcher contract.

Author Contributions

NO: Formal analysis, Investigation, Writing – original draft, Visualization. EMN: Formal analysis, Investigation, Writing – review & editing, Visualization. PD: Conceptualization, Supervision. MG: Project administration, Validation, Writing – review & editing. TRH: Conceptualization, Supervision, Project administration, Validation, Writing – review & editing.

Conflicts of interest

There are no conflicts to declare.

References

1 K. Sindelarova, C. Granier, I. Bouarar, A. Guenther, S. Tilmes, T. Stavrakou, J.-F. Müller, U. Kuhn, P. Stefani and W. Knorr, *Atmos. Chem. Phys.*, 2014, **14**, 9317–9341.

2 C. E. Scott, A. Rap, D. V. Spracklen, P. M. Forster, K. S. Carslaw, G. W. Mann, K. J. Pringle, N. Kivekäs, M. Kulmala, H. Lihavainen and P. Tunved, *Atmos. Chem. Phys.*, 2014, **14**, 447–470.

3 C. J. Hennigan, M. H. Bergin and R. J. Weber, *Environ. Sci. Technol.*, 2008, **42**, 9079–9085.

4 J. Thomas, O. Sukhorukov, W. Jäger and Y. Xu, *Angew. Chem. Int. Ed.*, 2014, **53**, 1156–1159.

5 C. Pérez, A. Krin, A. L. Steber, J. C. López, Z. Kisiel and M. Schnell, *J. Phys. Chem. Lett.*, 2016, **7**, 154–160.

6 E. M. Neeman, J. R. A. Moreno and T. R. Huet, *Phys. Chem. Chem. Phys*, 2021, **23**, 18137–18144.

7 T. Ausma and L. J. De Kok, *Front. Plant Sci.*, 2019, ***10***, 743

8 S. F. Watts, *Atmos. Environ.*, 2000, **34**, 761–779.

9 A. Das, P. K. Mandal, F. J. Lovas, C. Medcraft, N. R. Walker and E. Arunan, *Angew. Chem. Int. Ed.*, 2018, **57**, 15199–15203.

10 E. Arunan, T. Emilsson, H. S. Gutowsky, G. T. Fraser, G. de Oliveira and C. E. Dykstra, *J. Chem. Phys.*, 2002, **117**, 9766–9776.

11 M. Goswami and E. Arunan, *J. Mol. Spectrosc.*, 2011, **268**, 147–156.

12 E. M. Neeman and T. R. Huet, *Phys. Chem. Chem. Phys*, 2021, **23**, 2179–2185.

13 M. Chrayteh, E. Burevschi, D. Loru, T. R. Huet, P. Dréan and M. Eugenia Sanz, *Phys. Chem. Chem. Phys.*, 2021, **23**, 20686–20694.
14 M. Tudorie, L. H. Coudert, T. R. Huet, D. Jegouso and G. Sedes, *J. Chem. Phys.*, 2011, **134**, 074314.
15 H. M. Pickett, *J. Mol. Spectrosc.*, 1991, **148**, 371–377.
16 J. K. G. Watson, *Vib. Spectra Struct. Vol. 6. A Ser. Adv*, Elsevier, Amsterdam, 1977.
17 J. P. Foster and F. Weinhold, *J. Am. Chem. Soc.*, 1980, **102**, 7211–7218.
18 E. R. Johnson, S. Keinan, P. Mori-Sánchez, J. Contreras-García, A. J. Cohen and W. Yang, *J. Am. Chem. Soc.*, 2010, **132**, 6498–6506.
19 W. Humphrey, A. Dalke and K. Schulten, *J. Mol. Graph.*, 1996, **14**, 33–38.
20 E. G. Hohenstein and C. D. Sherrill, *J. Chem. Phys.*, 2010, **133**, 014101.